Journal of Nuclear Materials 390–391 (2009) 1149–1152

Contents lists available at ScienceDirect

Journal of Nuclear Materials

journal homepage: www.elsevier.com/locate/jnucmat

In situ reflectivity of tungsten mirrors under helium plasma exposure

W. Sakaguchi [a], S. Kajita [b,*], N. Ohno [a], M. Takagi [a]

[a] Department of Energy Engineering and Science, Nagoya University, Furo-Cho, Chikusa-Ku, Nagoya 464-8603, Japan
[b] EcoTopia Science Institute, Nagoya University, Furo-Cho, Chikusa-Ku, Nagoya 464-8603, Japan

ARTICLE INFO

PACS:
52.40.Hf
52.70.Kz
79.20.Ds
78.20.Ci

ABSTRACT

The formation of micron-sized helium bubbles/holes on tungsten surface due to helium ion irradiation has been investigated in the linear divertor plasma simulator NAGDIS-II [1]. In order to investigate the surface variation during the helium plasma exposure, the optical reflectivity is measured by using a He–Ne laser and a photodiode. When the incident helium ion energy is 15 eV, a great amount of bubbles and holes were formed by the exposure with the ion fluence of $1.8 \times 10^{27}\ m^{-2}$. The degradation of the reflectivity is enhanced when increasing the incident ion energy. When the incident ion energy is 30–50 eV, the surface is covered with fiberform nanostructured tungsten. The reflectivity recovery effect by a ruby laser with a long pulse duration of ~0.6 ms is demonstrated. The reflectivity recovers to the initial value when the laser pulse energy exceeds ~1.2 MJ m^{-2}.

1. Introduction

Divertor materials in fusion devices are exposed to high-density and low temperature deuterium–helium mixture plasmas. Tungsten (W) is one of the candidates for divertor materials in ITER because of its high thermal property and low sputtering yield [2]. Moreover, tungsten is considered as the candidate for in-vessel mirror materials for optical diagnostic systems in ITER [3]. One of the issues for the in-vessel mirrors and divertor materials is the effects of particle irradiations on the material properties. The effects of the irradiation of hydrogen isotopes to molybdenum, and W mirrors have been investigated [4]; and the decrease of the optical reflectivity of W by deuterium ion irradiation is less than 10% at fluence of $1.3 \times 10^{25}\ m^{-2}$. However, it is suspected that the irradiation effects of helium could be severer than that of hydrogen isotopes because of its strong interaction with the lattice defects. By helium plasma irradiation, it has been observed that bubbles and holes are formed on the tungsten surface even when the incident ion energy was less than the threshold energy of sputtering [5–9]. Under the other conditions, it has been reported that nanostructured tungsten is formed on tungsten surface [10,11]. These damages may cause the degradation of the thermophysical properties and optical reflectivity. From the viewpoint of the mirror material, it is important to investigate the effect of helium plasma irradiation on the optical reflectivity. In this paper, the change of the surface nature under helium plasma exposure is investigated by the measurement of the optical reflectivity and the surface analysis using a scanning electron microscope (SEM). Furthermore, the alleviation effect of the bubbles/holes by the irradiation of ruby laser pulses, the time duration of which corresponds to that of the edge localized modes (ELMs), is reported [12]. The effect of the irradiation of the ruby laser pulses on the optical reflectivity is shown.

2. Experimental setup

Fig. 1 shows the schematic view of the experimental setup in the divertor plasma simulator NAGDIS-II. Steady state high-density plasma is produced by a dc arc discharge using a LaB_6 cathode heated with a filament. The magnetic field strength was 0.1 T. The specimen was powder metallurgy tungsten provided by Nilaco Co. with 99.95% purity and 0.2 mm in thickness. Samples were polished to a mirror finish. In order to control the incident ion energy to the samples, they were electrically biased in some experiments. The space potential was ~−1 V, which was sufficiently smaller than the biasing voltage. The reflectivity of specimen was measured by using a He–Ne laser, whose wavelength is 632.8 nm, and a photodiode with a band-pass optical filter to exclude the emission from the plasma. The surface temperature of the samples was measured by a pyrometer and the surface modification was observed by SEM. For a transient heat source, a ruby laser (Nihon Kosyuha: SLP2005) without a Q-switch was used. The wavelength, pulse width, and pulse energy were, respectively, 694 nm, 0.6 ms, and ~5 J. The laser diameter at the target was approximately 1.0 mm.

* Corresponding author.
E-mail addresses: w-sakaguchi@ees.nagoya-u.ac.jp (W. Sakaguchi), kajita@ees.nagoya-u.ac.jp (S. Kajita).

0022-3115/$ - see front matter © 2009 Elsevier B.V. All rights reserved.
doi:10.1016/j.jnucmat.2009.01.276

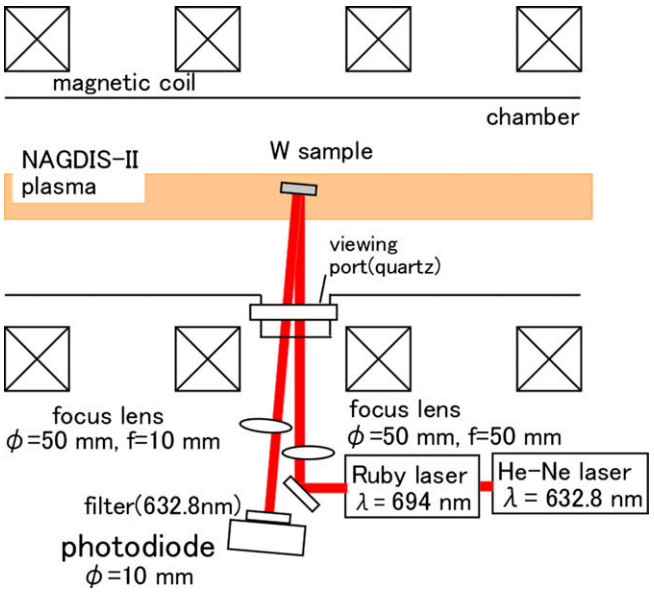

Fig. 1. Schematic illustration of the experimental setup in the divertor simulator NAGDIS-II. He–Ne laser is used for measuring optical reflectivity of the sample, and ruby laser is used for a transient heat source.

3. Results and discussion

3.1. In situ reflectivity measurement of tungsten under helium plasma exposure

Fig. 2 shows the optical reflectivity of samples exposed to the helium plasma, the electron temperature T_e and density n_e of which were 7 eV, and 1.2×10^{19} m^{-3}, respectively. In case 1, the sample was at the floating potential of −15 V (W1). In cases 2, 3, and 4, the samples were biased to −30 V (W2), −50 V (W3), and −80 V (W4), respectively. The exposure conditions are summarized in Table 1. The ion flux was evaluated by measuring the ion current to the sample in cases 2–4, while in case 1, the ion flux could not be evaluated because W1 was at the floating potential; the ion flux in case 1 may be slightly less than that in case 2. In cases 1 and 2, the reflectivity decreases during several hours; on the other hand, the reflectivity decreases during much shorter period of time in cases 3 and 4. Even though the ion flux did not change so much in these four cases, the reduction time in reflectivity decreases significantly with increasing the incident ion energy. Although the surface temperature slightly increases with the incident ion energy, it is likely that the surface damages strongly depend on the incident ion energy.

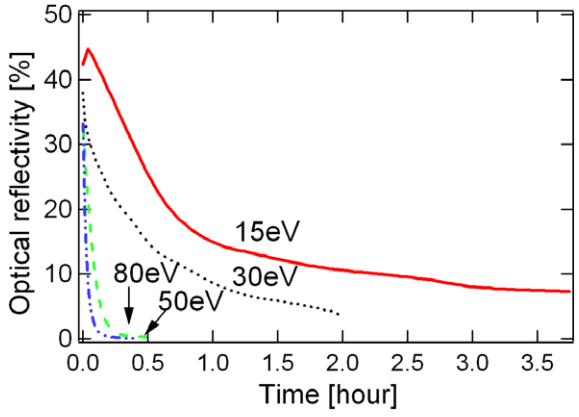

Fig. 2. Measured optical reflectivity of tungsten under helium plasma exposure; the detail exposure conditions are summarized in Table 1.

Fig. 3(a)–(f) shows the SEM micrographs of the samples after the helium plasma exposure. Helium bubbles and holes are formed on the W1 surface (Fig. 3(a)). From W1 in Fig. 2, it can be said that a great amount of bubbles/holes are formed by the exposure during one hour. Concerning W2, and W3, the surface color was totally black visually after the exposure. The surfaces of W2, and W3, are covered with a sub-micrometer fine structured material shown in Fig. 3(b)–(d). A lot of nanosized rods are disorderly connected. On the other hand, no nanosized rods are observed on the W4 surface, as shown in Fig. 3(e) and (f); but globular shaped structure is observed. From the visual observation, the surface color of W4 was not black after the exposure. The high surface temperature of W4 might suppress the nanosized rods formation.

Fig. 4 shows the wavelength dependence of the specular reflectivity of the unirradiated polished sample and the samples exposed to helium plasma (W1, W3, and W4). The reflectivities at 632.8 nm are consistent with the in situ measurement results of the optical reflectivity. As for W1, the reflectivity decreases by an order of magnitude at 300 nm, though it decreases to half the initial value at 900 nm. The reduction degree in reflectivity is more significant when the wavelength is shorter. Concerning W3 and W4, the reflectivity is almost zero in this wavelength range.

3.2. Recovery of optical reflectivity by heat pulse

Fig. 5 shows SEM micrograph of sample after the ruby laser irradiation under helium plasma exposure. In the left part of Fig. 5, where the laser pulses were irradiated, the bubbles/holes disappeared. The mechanism of the alleviation of bubbles/holes is discussed in Ref. [12]; it is indicated from the calculation of the surface temperature that the surface damage is alleviated by the recrystallization process.

Fig. 6 shows the reflectivity of W1 sample at the position where the ruby laser pulses were irradiated during the helium plasma exposure. The sample W1 was pre-exposed to helium plasma during ~3.7 h, as shown in Fig. 2; thus, a lot of bubbles/holes were formed on the surface before the laser pulse irradiation. Five ruby laser pulses were irradiated to the same position. The laser pulse energies at the first and second pulses were 1.7 MJ m^{-2}, while the pulse energies of third to fifth pulses were 0.6 MJ m^{-2}, 0.8 MJ m^{-2}, and 1.2 MJ m^{-2}, respectively. It is worthwhile to note that the heat load is close to that of the type-I ELMs of ITER, the

Table 1
Experimental parameters of the helium irradiation experiment for W1, W2, W3, and W4.

	W1	W2	W3	W4
Incident ion energy	15 eV	30 eV	50 eV	80 eV
Fluence	–	6.3×10^{26}/m^2	1.7×10^{26}/m^2	3.3×10^{26}/m^2
Ion flux	–	5.8×10^{22}/m^2 s	7.5×10^{22}/m^2 s	9.2×10^{22}/m^2 s
Time	36000 s	10800 s	2300 s	3600 s
Temperature	1780 K	1800 K	1890 K	2100 K
Surface modification	He bubble/hole formation	Fiberform nanostructure	Fiberform nanostructure	

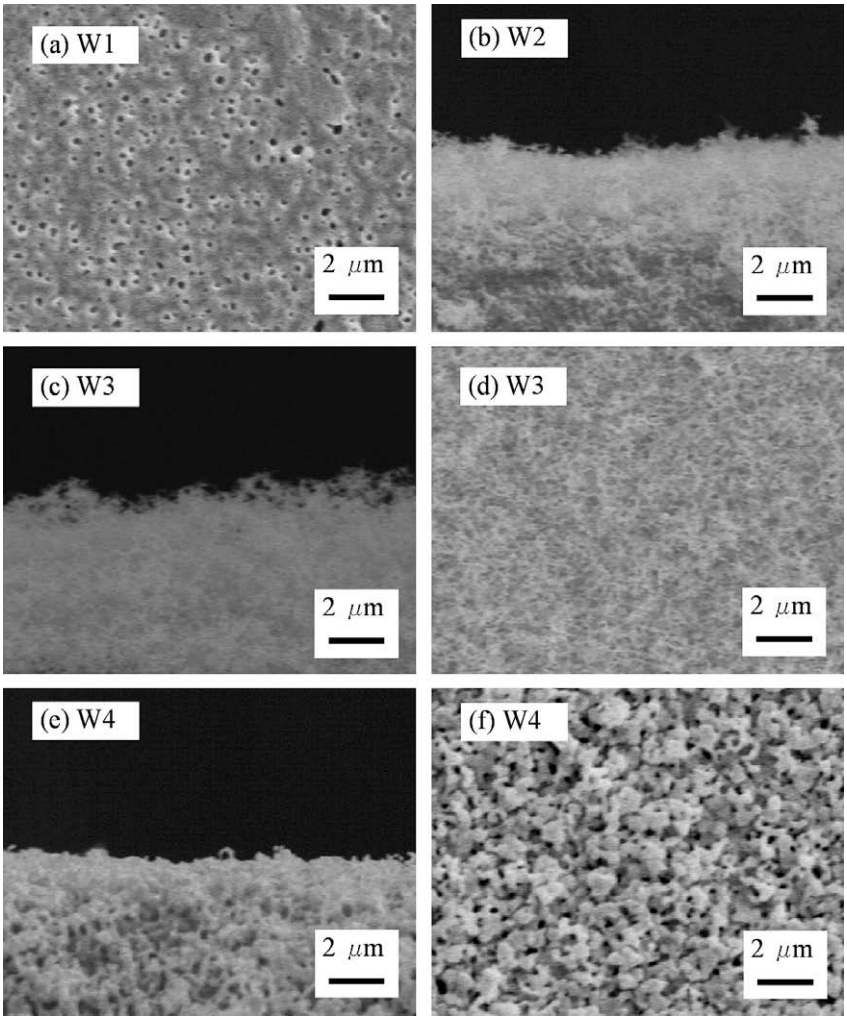

Fig. 3. SEM micrographs of tungsten surface exposed to helium plasma. (a), (d), and (f) are at the center of samples, (b), (c), and (e) are at the edge of samples from top view.

heat load of which is expected to be 0.2–2.0 MJ m^{-2} with the duration of 0.1–1 ms. The optical reflectivity is recovered to approximately 40% which is almost the initial value, when the laser pulse energy exceeds 1.2 MJ m^{-2}. This clearly demonstrated the effects of the transient heat load on a reflectivity recovery. The degree of the reflectivity recovery effect depends on the laser pulse energy when the pulse energy is less than 1.2 MJ m^{-2}. It is noted that the reduction time in reflectivity does not change from the virgin sample after the ruby laser irradiation. The laser irradiation experiments for the damaged tungsten such as W2–W4 are currently underway and remained as a future work.

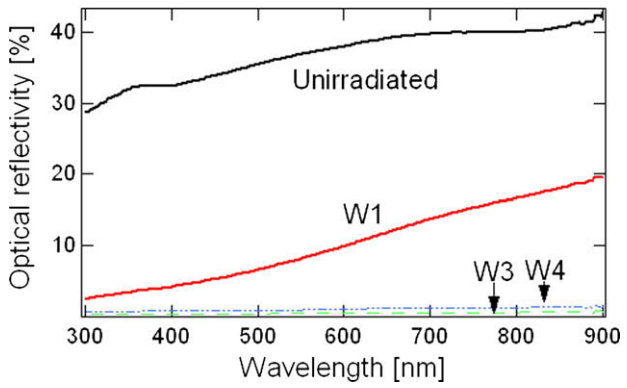

Fig. 4. Specular reflectivity of the unirradiated polished sample and the samples exposed to helium plasma.

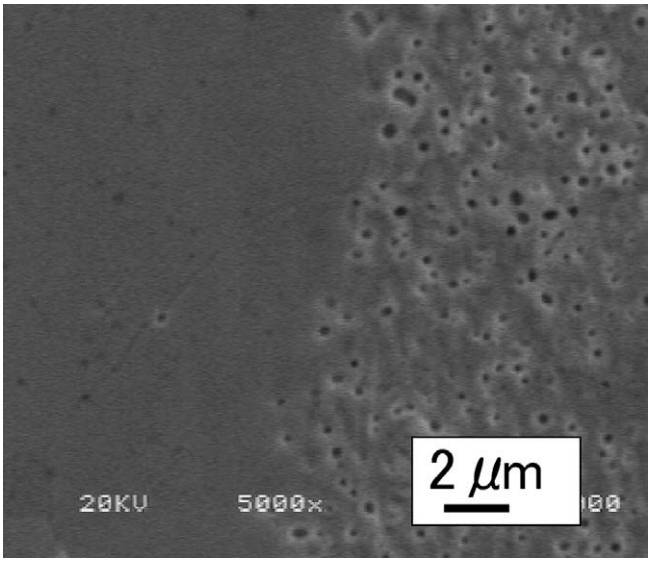

Fig. 5. SEM micrograph of tungsten surface exposed to ruby laser under helium plasma exposure. The right and left parts correspond to the position without and with ruby laser irradiation, respectively.

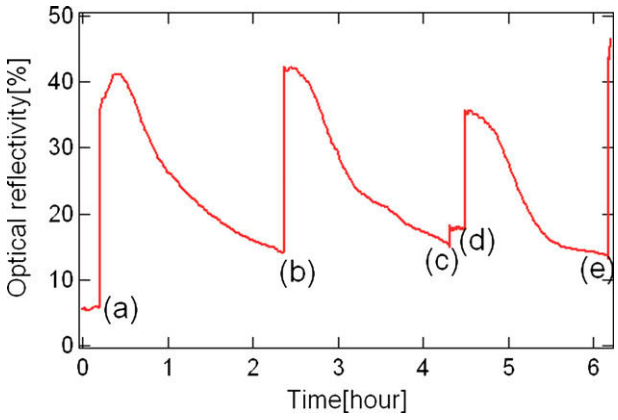

Fig. 6. Measured optical reflectivity of tungsten under helium plasma exposure at the floating potential. Five ruby laser pulses are irradiated. The laser pulse energies are (a) 1.7 MJ m^{-2}, (b) 1.7 MJ m^{-2}, (c) 0.6 MJ m^{-2}, (d) 0.8 MJ m^{-2}, and (e) 1.2 MJ m^{-2}.

4. Conclusions

We have investigated the effects of bubbles/holes, which are formed on tungsten surface due to the helium plasma exposure, on the optical reflectivity. The optical reflectivity of tungsten decreased significantly by the exposure to the helium plasma. The characteristic time of the reflectivity reduction decreased with the incident ion energy by approximately an order of magnitude. When the incident ion energy was 15 eV, bubbles/holes were formed on the surface. On the other hand, when the incident ion energy was 30–50 eV, the surface was covered with fiberform nanostructured materials. It is indicated that the incident ion energy is an important parameter to form fiberform nanostructured tungsten. From the view point of divertor material, the formation of nanosized rods should be prevented by controlling those parameters.

Moreover, we confirmed the recovery effect of the optical reflectivity by the laser heat pulse, which has almost same pulse duration of ELMs. The alleviation effect of bubbles/holes can be applied to in situ mirror cleaning.

Acknowledgements

This research was partially supported by the Ministry of Education, Science, Sports and Culture, Grant-in-Aid for Scientific Research (B), 19360413. This work also was supported in part by a Grant-in-Aid for Young Scientists (Start-up), 19860096, from the Japan Society for the Promotion of Science (JSPS). Authors are deeply grateful to Dr. Tokitani from NIFS for his experimental support.

References

[1] S. Takamura, N. Ohno, D. Nishijima, Y. Uesugi, Plasma Sources Sci. Technol. 11 (2002) A42.
[2] ITER Physics Basis, Nucl. Fus. 39 (1999) 2137.
[3] A. Litnovsky, V.S. Voitsenya, A. Costley, A.J.H. Donne, Nucl. Fus. 47 (2007) 833.
[4] T. Sugie, S. Kasai, M. Taniguchi, et al., J. Nucl. Mater. 329–333 (2004) 1481.
[5] M.Y. Ye, S. Takamura, N. Ohno, J. Nucl. Mater. 241–243 (1997) 1243.
[6] M.Y. Ye, N. Ohno, S. Takamura, J. Plasma Fus. Res. 3 (2000) 265.
[7] D. Nishijima, M.Y. Ye, N. Ohno, S. Takamura, J. Nucl. Mater. 313–316 (2003) 99.
[8] D. Nishijima, M.Y. Ye, N. Ohno, S. Takamura, J. Nucl. Mater. 329–333 (2004) 1029.
[9] N. Yoshida, H. Iwakiri, K. Tokunaga, T. Bada, J. Nucl. Mater. 337–339 (2005) 946.
[10] S. Takamura, N. Ohno, D. Nishijima, S. Kajita, Plasma Fus. Res. 1 (2006) 051.
[11] M.J. Baldwin, R.P. Doerner, Nucl. Fus. 48 (2008) 035001.
[12] S. Kajita, S. Takamura, N. Ohno, et al., Nucl. Fus. 47 (2007) 1358.